# ANALYSIS OF WIND FLOW DIVERTING AND ACCELERATING CHARACTERISTICS OF POROUS AND NON-POROUS CIRCULAR OBSTACLES

Abdul Latif Manganhar*, Muhammad Ramzan Luhur*, Altaf Hussain Rajpar**, Saleem Raza Samo**

## ABSTRACT

**Structures and tall buildings in urban environment have been considered responsible factors for generating turbulence and reducing velocity of the wind flow. Thus, the decisions about positioning the wind turbines in urban areas require several factors to consider. Literature review reflects that the wind flow diverting and accelerating characteristics of existing obstacles are less attended. In the present study, wind velocity variations taking place in the exterior local environment of porous and non-porous obstacles (except over the obstacle) are analyzed. To analyze the resulting wind flow characteristics, the simulations have been carried out using ANSYS Fluent, CFD code. The results reflect that optimum velocity magnitude can be achieved in the diverted paths at left and right sides of the obstacles.**

*Key words:* wind flow diversion, wind flow acceleration, turbulent flow, porous obstacle, non-porous obstacle, CFD.

## 1. INTRODUCTION

The energy dependent socio-economic development processes, increasing population and energy demand, insufficient and fossil fuel based power generation are the most critical energy concerned issues of the world. Utilization of fossil fuels as energy resource not only contributes to environmental pollution but deplete also [1-4]. In the light of these issues following areas are required to be focused:

- more power generation
- small scale and indigenous technology
- most effective and economical systems
- exploitation of renewable and indigenous environment friendly resources [5-8].

For the built environment, micro generation technology is the preferable choice. In contrast to the traditional centralized energy supply, micro technologies bring power generation close to the user to sustain their buildings. To utilize this technology, estimations suggest a huge potential in the urban environment not only to satisfy the demand and provide the decentralized generation, but also to tackle the fuel shortage as well as to achieve the reduction in emissions [9].

Nevertheless, the developments in the direction of micro technology are limited due to quality of the wind flow in these zones [10]. The observations manifest that the performance of a building mounted wind turbine is strongly dependent on site selection. Further, the site measurements of wind speed require time and money, which are often not available for micro projects [11].

Therefore, sites selected for small scale wind turbines in built environment are often roofs of tall buildings, where less turbulent wind is available.

All structures have aerodynamic characteristics and modify wind flow in their local-environment. These modifications may or may not be beneficial for the locations where the structure exists. Literature reveals the study of roof top small scale wind turbine characteristics, nevertheless, the characteristics of such installations at other sides of the building are less investigated.

In the present study wind velocity variations taking place in the exterior local environment of porous and non-porous obstacles (except over the obstacle) are taken into consideration. The simulations are performed using the ANSYS Fluent CFD code to identify the velocity variations and optimum accelerated locations in the diverted flow.

The paper is organized such that Section 2 describes the material and methods, Section 3 presents the results and discussions and the last Section 4 concludes the outcome.

## 2. MATERIALS AND METHODS

In order to specify the wind flow variations, two circular obstacles, i.e., one solid (non-porous) and other porous having identical dimensions with swept area of $0.24$ m$^2$ were considered, as shown in Figure 1. The solid obstacle is a circular cylinder of diameter 0.8 m and height 0.3 m, and the porous obstacle is a circular structure of same size with four walls tilted at angle of 45$^{\circ}$. The porous structure provides several paths for wind to flow through it.

---

*Assistant Professor, Quaid-e-Awam University of Engineering, Science and Technology, Nawabshah, Pakistan.

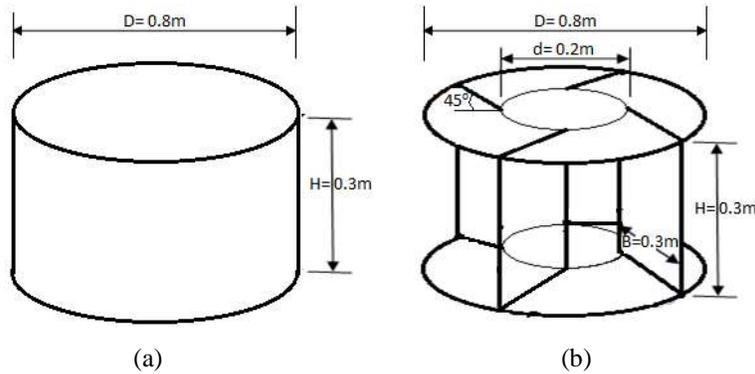**Professor, Quaid-e-Awam University of Engineering, Science and Technology, Nawabshah, Pakistan.

(a)                                      (b)

Figure-1: Obstacles to wind flow, (a) solid obstacle and (b) porous obstacle

## 2.1. CFD SIMULATIONS

The CFD simulations are performed using the student version of Ansys fluent 14.5. The flow behavior over the obstacles (described in Section 2) is analyzed through RANS model; the SST K-ω at wind speed of 5 m/s. The computational domain for present simulations is given in Figure 2, where diameter D is 0.8 m. The boundary conditions for this domain are described in Table 1. The meshing for computational domain was performed using Quad/Tri:Pave meshing scheme.

**Table 1: Wall boundary conditions**

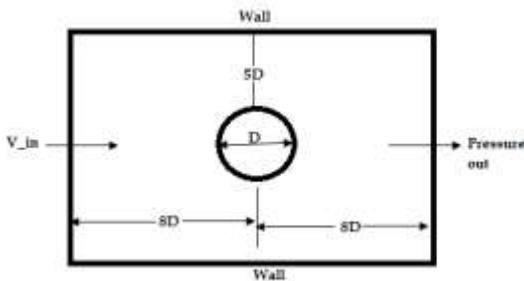| Inlet boundary conditions | | Outlet boundary conditions | |
|---|---|---|---|
| **Type** | **Velocity inlet** | **Type** | **Pressure outlet** |
| Reference Frame | Absolute | Gauge pressure | 0 |
| Coordinate System | Cartesian | Backflow direction specification method | Normal to boundary |
| X-Velocity (m/s) | 5 | Turbulence specification method | K and Omega (SST) |
| Y-Velocity (m/s) | 0 | Backflow turbulent intensity (%) | 5 |
| Z-Velocity (m/s) | 0 | Back flow turbulent viscosity ratio | 10 |
| Turbulence specification method | K and Omega (SST) | - | - |
| Turbulent intensity (%) | 5 | - | - |
| Turbulent viscosity ratio | 10 | - | - |



Figure-2: Computational domain for simulations.

## 2.2. THEORETICAL ANALYSIS

The wind at the entrance of a path between two buildings becomes compressed, where pressure increases and velocity decreases. However, after entering (wind flow) into the mentioned path, the flow velocity increases due to pressure difference between the upstream and downstream sides of the buildings. According to Bernoulli's principle, the wind speed along a path between two obstacles increases considerably [12].

Here, we place a circular obstacle into a flow channel as shown in Figure 3, where $A_1$ represents the upstream wind channel cross-sectional area at Section 1 and $A_2$ the cross-sectional area at Section 2. The cross-sectional area at Section 2 reduces due to existence of an obstacle in flow path. According to Bernoulli's principle:

$$A_1 V_1 \rho_1 = A_2 V_2 \rho_2 = \text{constant} \qquad (1)$$

Where $V_1$ and $V_2$ are the flow velocities, and $\rho_1$ and $\rho_2$ are fluid densities at Sections 1 and 2, respectively. For low wind speeds, i.e., less than 100 m/s, the change in density is negligible [13]. In this context, equation (1) can be written as:

$$V_2 = (A_1/A_2) V_1 \qquad (2)$$

Equation (2) reflects that for any contraction ratio $(A_1/A_2) > 1$, there is increase in $V_2$. This local increase in flow velocity is contributed by the obstacle.
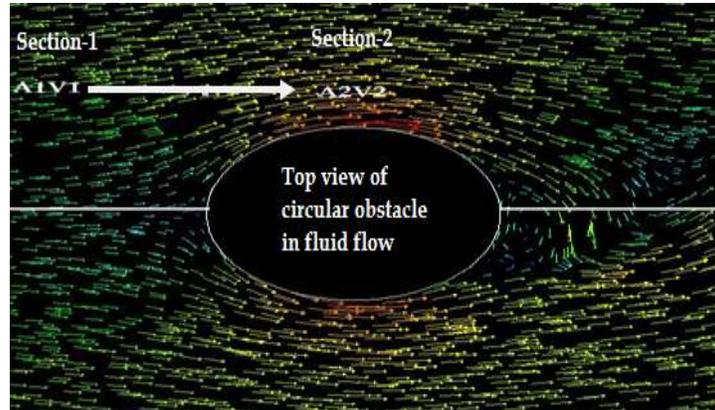


Figure-3: Two-dimensional view of a circular obstacle in a flowing fluid in CFD.

The focus of present research work is to study the magnitude of diverted flow, increase in flow velocity and the location of optimum velocity with turbulent level.

## 3. RESULTS AND DISCUSSIONS

### 3.1. Solid Circular Obstacle

To understand the effects of obstacle on wind flow and to determine the optimum velocity location in the new flow path, both the turbulence intensity and the magnitude of velocity (in stream wise direction) were analyzed. The obstacle effect on the wind flow can be visualized clearly through velocity vectors and contour lines, as shown in Figure 4, which reflect the asymmetric flow due to blockage effect of the obstacle. The flow experiences the compression effect which causes reduction in velocity as it comes closer to obstacle. The flow diverts the path following the wall of obstacle (here wall of the obstacle reduces the flow channel width and creates venturi effect) and accelerates at either side of the obstacle.
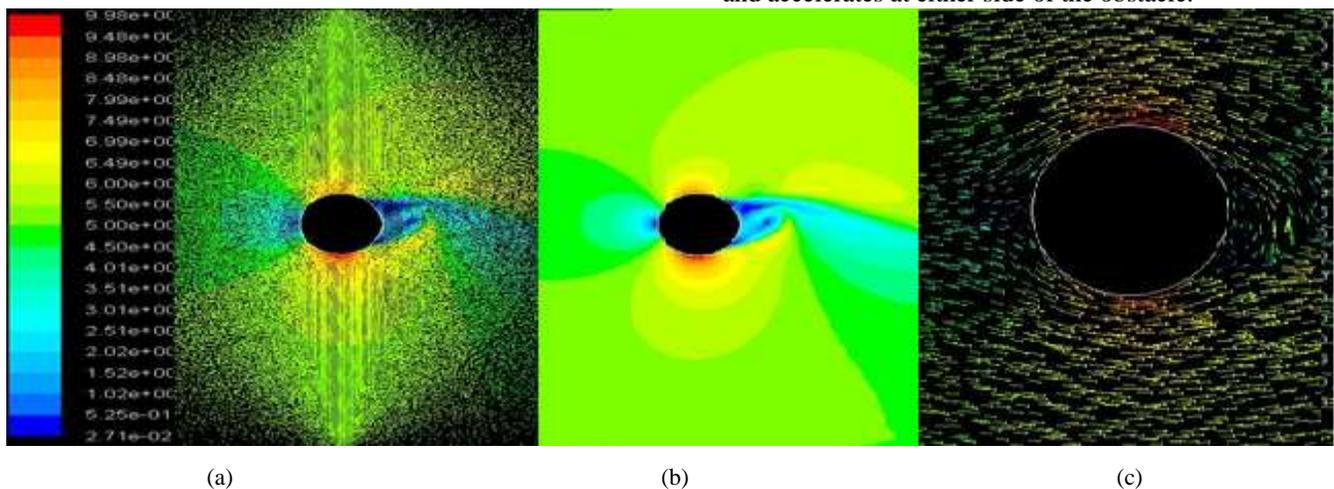


(a)            (b)            (c)

Figure-4: Vectors and contours showing variations in wind velocity magnitude experiencing a solid circular obstacle in its flow path. (a, c) Vectors and (b) contours.

For the width of flow which is equal to D/4, five streamlines passing through the points P(0,40), P(0,45), P(0,50), P(0,55) and P(0,60) have been considered to observe the effect of obstacle on their velocity. The variations in velocity magnitude along the flow channel are shown in Figure 5, which shows an increase of 4 m/s in upstream wind flow. In other words 5 m/s free stream wind velocity approaches to approximately 9 m/s close to the obstacle P(0,40) after a thin boundary layer.

The magnitude of velocity decreases with increase in width of flow from the obstacle. The streamline passing close to the obstacle achieves maximum velocity of 9 m/s at P(0,40), and the streamline passing at a distance of D/4 from the obstacle achieves maximum velocity of 7 m/s at

P(0,60) as shown in Figure 5. The average velocity magnitude in the selected flow width is approximately 8 m/s, which is an average increase of 62.5% in the free stream flow velocity.

Further, to investigate the flow quality at this location, turbulent intensity and turbulent kinetic energy are estimated given in Figure 6. The contours of turbulent intensity and turbulent kinetic energy exhibit asymmetric behavior of the flow due to same reason described for Figure 4. The figure, for specific considered width of the flow, indicates uniform flow with turbulent intensity of nearly 1% and turbulent kinetic energy less than 0.25 $m^2/s^2$.
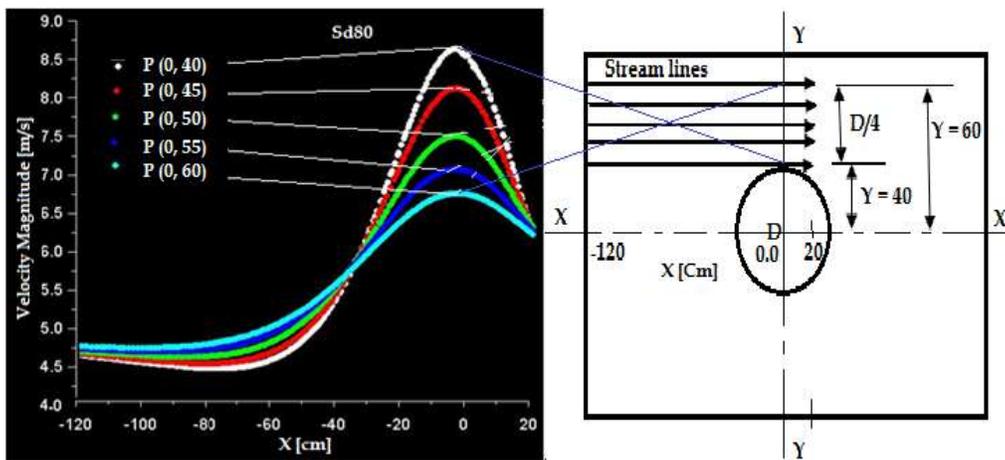


Figure-5: Variations in wind velocity magnitude along five horizontal lines (at Y = 40, 45, 50, 55, 60 cm) drawn parallel to each other in stream wise direction at left side of the solid obstacle.
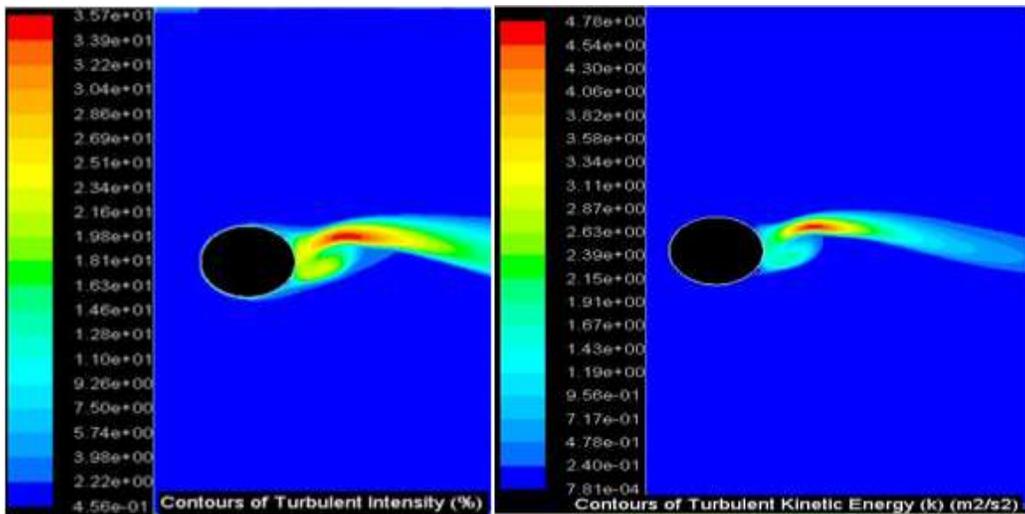


Figure-6: Contours of turbulent intensity and turbulent kinetic energy showing quality of flow around the solid circular obstacle.

## 3.2. POROUS CIRCULAR OBSTACLE

The velocity vectors and contours for porous circular obstacle are shown in Figure 7, which exhibit almost

similar behavior of wind flow as it was observed for solid circular obstacle (see Figure 6). The cross sectional area of wind flow, which is equal to the projected area of

obstacle, interacting with obstacle structure, follows the paths available inside the structure. Here, flow also experiences the compression effect and reduction in wind velocity close to the obstacle as observed in solid circular obstacle case. Nevertheless, being porous obstacle, it allows part of the flow to pass through it. The rest of the flow diverts the path, concentrates and accelerates at either side of the obstacle like in solid obstacle case.
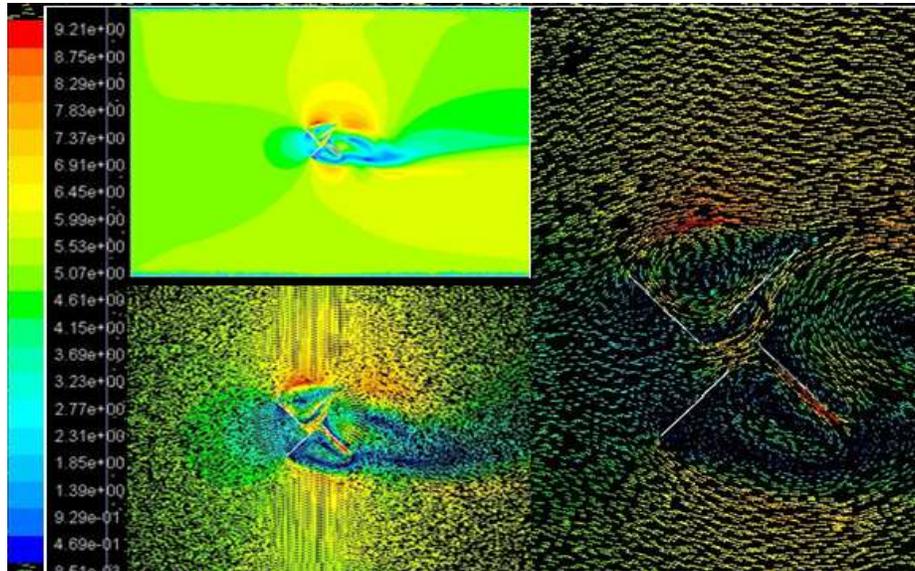


Figure-7: Vectors and contours showing variations in wind velocity magnitude experiencing a porous circular obstacle in its flow path.

Similarly, as in solid obstacle case, the magnitude of velocity decreases with increase in width of flow from the obstacle. The maximum velocity close to obstacle at P(0,40) is approximately same 9 m/s, which decreases to 7.4 m/s at distance D/4 at P(0,60) away from the obstacle, as shown in Figure 8. The average velocity magnitude in the selected flow width is approximately 8.2 m/s, which is an average increase of 64% in the free stream flow velocity. Figure 9 describes the quality of flow around a porous circular obstacle. Similarly, the contours of turbulent intensity and turbulent kinetic energy, here also exhibit asymmetric flow behavior (for the same reason as described for Figures 4 and 6) for the porous obstacle as observed for solid obstacle. Further, the turbulent intensity is approximately 2%, whereas the turbulent kinetic energy is less than 0.25% (see Figure 9). The values represent the spatial average, which can be read from status bar of the Figure 9. Summarizing, the changes in parameters reflect similar behavior in both cases, except slight variations in their magnitudes.
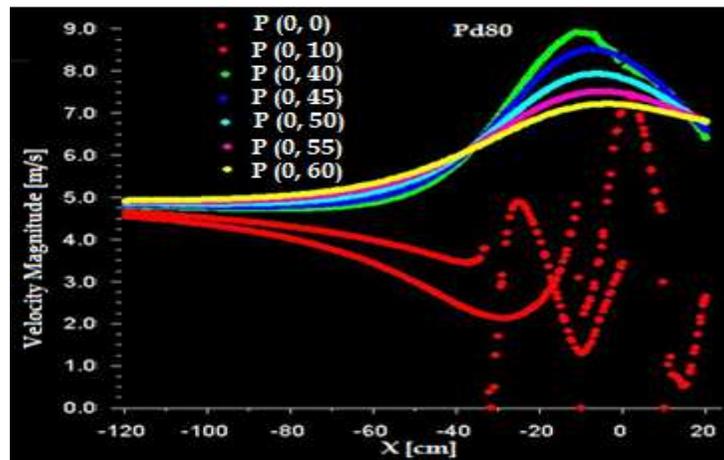


Figure-8: Variations in wind velocity magnitude for seven streamlines in the stream-wise direction passing through the center as well as from left side of the porous obstacle.

The variations in velocity ratio contributed by both obstacles are indicated in Figure 10. The figure reflects nearly similar behavior for wind flow around the porous and non-porous structures having identical exterior dimensions. The results manifest that such obstacles play a vital role for accelerating wind passing around them.
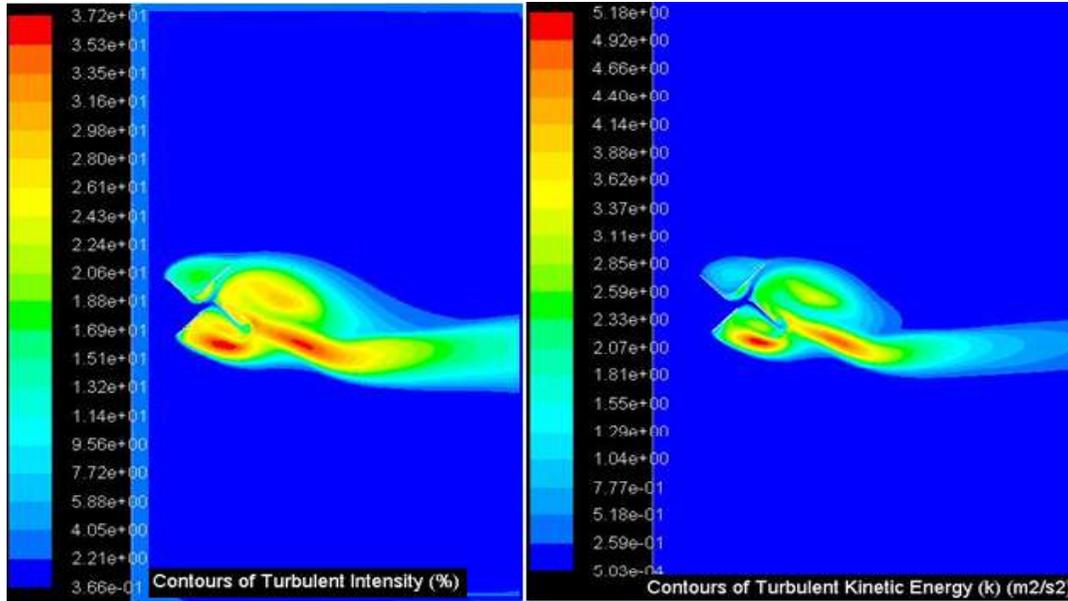


Figure-9: Contours of turbulent intensity and turbulent kinetic energy showing quality of flow around a porous circular obstacle.
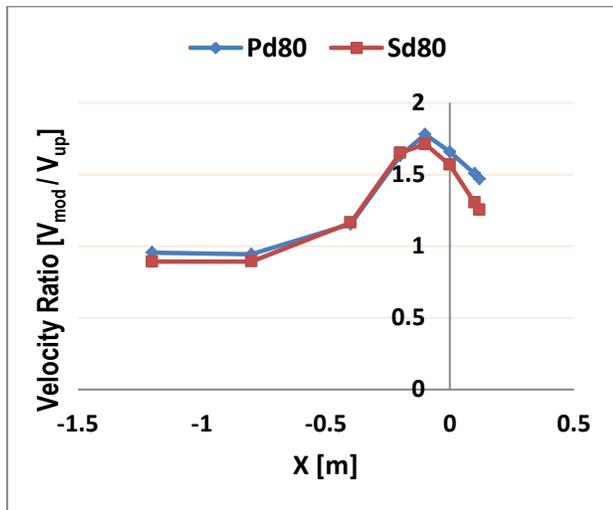


Figure-10: The variations in wind velocity ratio contributed by both porous (Pd80) and solid (Sd80) obstacles describing the behavior of wind passing around them. Here $V_{mod}$ and $V_{up}$ represent the modified and upstream flow velocities, respectively.

## 4. CONCLUSION

The wind velocity variations in the exterior local environment of porous and non-porous circular obstacles (except over the obstacle) have been analyzed using CFD simulations.

The magnitude of velocity decreases with increase in width of flow from an obstacle. For both obstacles, the maximum increase in the velocity over 5 m/s upstream wind is 4 m/s (i.e. increased from 5 m/s to 9 m/s) close to the obstacle after the thin boundary layer. At distance of D/4 from the obstacle, the flow velocity decreases to 7 m/s in case of solid obstacle and 7.4 m/s in case of porous obstacle. The average velocity magnitudes in the selected flow width (D/4) are approximately 8 m/s (increase of 62.5%) and 8.2 m/s (increase of 64%), respectively, for solid and porous obstacles. The turbulent intensity is approximately 1% in case of solid obstacle and 2% in case of porous. The turbulent kinetic energy is identical for both obstacles, which is less than 0.25 $m^2/s^2$.

Summarizing, the changes in parameters reflect similar behavior in both cases, except slight variations in their magnitudes. For both the obstacles, flow experiences the compression and reduction in velocity as it comes closer to the obstacle. Further, flow diverts the path, concentrates and accelerates at either side of the obstacle.

## REFERENCES

[1] "Fossil fuel overview", Ministry of Petroleum and Natural Resources Pakistan, 2005.

[2] Khanji H, Uqaili M.A and Memon M, "Renewable Energy for Managing Energy Crisis in Pakistan", IMTIC: 449-455, 2008.

[3] "Pakistan Statistics", International Energy Agency (IEA), 2007.

[4] Sheikh M.A, "Energy and renewable energy scenario of Pakistan", Renewable and Sustainable Energy Reviews, Vol. 14, pp. 354–363, 2010.

[5] Islam M, "Design and Development of a Vertical Axis Micro Wind Turbine", Master thesis, University of Manchester, UK, 2010.

[6] Eriksson S, Bernhoff H and Leijon M, "Evaluation of Different Turbine Concepts for Wind Power", Renewable and Sustainable Energy Reviews, Vol. 12, pp. 1419-1434, 2008.

[7] Wagner H and Mathur J, "Introduction to Wind Energy Systems", Springer, Germany, ISBN 978-3-642-02022-3, 2009.

[8] Mathew S, "Wind Energy: Fundamentals, Resource Analysis and Economics", Springer, Berlin, 2006.

[9] "Potential for micro generation study and analysis", Final Report, November 14, 2005.

[10] Bahaj A.S, James P.A.B, "Urban energy generation: the added value of photovoltaics in social housing", Renewable and Sustainable Energy Reviews, Vol. 11, No. 9, pp. 2121-2136, 2007.

[11] Walker S.L, "Building mounted wind turbines and their suitability for the urban scale-A review of methods of estimating urban wind resource", Energy and Buildings, Vol. 43, pp. 1852–1862, 2011.

[12] Ragheb M, "OROGRAPHY AND WIND TURBINE SITING", 2015.

[13] http://www.cfd-online.com/Forums/main/8344-incompressible-compressible-flow.html, accessed June 16, 2015.